Environmental Science Advances

ROYAL SOCIETY OF CHEMISTRY

PAPER

View Article Online
View Journal | View Issue

Cite this: *Environ. Sci.: Adv.*, 2023, **2**, 1554

A porous bentonite–coconut husk composite for the enhanced adsorption of selected emerging contaminants from aqueous solution

Abisola O. Egbedina, *[a] Simisola B. Odejobi,[a] Babatunde J. Akinbile,[b] Abayneh A. Ambushe,[b] Bamidele I. Olu-Owolabi[a] and Kayode O. Adebowale[a]

The preparation of bentonite clay–coconut husk composite (BECH) *via* microwave-assisted carbonization, the activation of BECH with HCl (BECH-H) and KOH (BECH-K) and the adsorption of ciprofloxacin, tetracycline, and bisphenol A from aqueous solutions by the resultant carbon materials are highlighted in this study. The adsorbents (BECH, BECH-H and BECH-K) were characterised by transmission electron microscopy, scanning electron microscopy, energy dispersive X-ray spectroscopy, Fourier transform infrared spectroscopy, X-ray diffraction and N_2 adsorption–desorption analysis using the BET model. The results from these analyses showed sufficient interactions between bentonite and coconut husk. The adsorbents exhibited high specific surface areas (284–456 $m^2\ g^{-1}$) showing potential to be used in adsorption studies. The Sips model provided the best fit to the adsorption data when data from the equilibrium experiment were fitted to the Freundlich and Sips models. BECH-H and BECH-K demonstrated the highest affinity for bisphenol A with BECH-H having the highest adsorption capacity (472.9 mg g^{-1}). BECH also had the greatest preference for the adsorbents, having adsorption capacities of 199.7 mg g^{-1} for ciprofloxacin, 183.5 mg g^{-1} for bisphenol A and 281.7 mg g^{-1} for tetracycline. Results showed high removal efficiencies for the ECs studied (>90%) at a low dosage of the adsorbents (50 mg). The kinetic data of all the adsorbents are best described by the pseudo-second-order kinetic model. Adsorption reactions were heterogeneous in nature with chemisorption being the rate-limiting step. These findings suggest that these adsorbents could be excellent materials for effectively treating EC-contaminated water.

Received 11th February 2023
Accepted 5th August 2023

DOI: 10.1039/d3va00033h

rsc.li/esadvances

Environmental significance

Emerging contaminants in the environment are sources of concern because their presence has been linked to diseases such as cancer, neurological problems and an increase in antibacterial resistance in microorganisms. Wastewater treatment plants are incapable of removing these contaminants. Several kinds of research on adsorption have focused on the search for low-cost, environmentally friendly adsorbents. This study presents an adsorbent synthesized from bentonite and coconut husk both of which are abundant, low-cost and non-toxic. This composite overcomes the deficiencies of the parent materials and is effective for the removal of ciprofloxacin, tetracycline and bisphenol A from water.

1. Introduction

Pharmaceuticals and plasticizers are two examples of emerging contaminants (ECs), which are prevalent in large concentrations in the environment but not regulated yet. They have also been reported to have detrimental effects on human health and the environment.[1]

Bisphenol A is one emerging contaminant that has drawn significant attention from the international community. With an annual production of 2.2 million tonnes of BPA in 2009, it is a chemical that is found in a variety of products including food contact materials, household kitchenware, cans, medical equipment and toys due to its ability to improve the durability, shatter resistance and heat resistance of plastics.[2] Bisphenol A was added to the candidate list of Substances of Very High Concern (SVHC) by the European Chemicals Agency in 2017 because of its harmful effects on humans.[3] These effects include imitating or suppressing the functions of the body's natural hormones which can interfere with the normal function of the reproductive system. Abnormalities in the sex organs, sperm quality, fertility, endometriosis, and early puberty have all been connected to reproductive system dysfunction. Exposure to

[a]*Department of Chemistry, University of Ibadan, Nigeria. E-mail: ao.egbedina@ui.edu.ng*

[b]*Research Centre for Synthesis and Catalysis, Department of Chemical Sciences, University of Johannesburg, South Africa*

bisphenol A has also been linked to the feminization of fish even at low concentrations in aquatic habitats.[4,5]

Tetracycline conversely is a broad-spectrum antibiotic that works against several Gram-positive and -negative bacteria and therefore widely used to treat infections with insignificant side effects. Tetracycline is also added to animal diets to encourage their growth and this makes it the second most produced and consumed antibiotic in the world[6,7] and ciprofloxacin is the fluoroquinolone antibiotic that is most widely used worldwide.[8] Unfortunately, antibiotics are only partially biodegradable and are not completely absorbed by both humans and animals.[9] Owing to their difficulty in degrading, antibiotics accumulate in the environment[10] and are known to increase the risk of cancer, have genotoxic and mutagenic effects, impact the immune, nervous and respiratory functions, and cause metabolic dysfunctions, diabetes, cardiovascular disorders, and neurological and learning problems. Furthermore, it has been demonstrated that microorganisms become more resistant to antibiotics when pharmaceutical residues are present in the environment.[11,12]

Emerging contaminants can enter the environment from point sources such as wastewater treatment plants or non-point sources such as agriculture.[13–15] They have been found in groundwater and surface water as well as being detected in food, plants and soils.[14,15] Emerging contaminants in wastewater have been eliminated using advanced oxidation processes (AOPs) and membrane processes.[16] These methods do, however, have drawbacks including prohibitive operating costs,[17] partial mineralization/rejection, and secondary pollution.[18]

Adsorption, on the other hand, is appealing because it is a flexible, effective and less expensive alternative.[11,19,20] It is also simple to integrate into existing wastewater treatment systems.[21] Several adsorbents have been developed for the removal of antibiotics such as activated carbon[22,23] clays,[24,25] biomass including chitosan, corn cob, banana peel, coffee husk[26–29] and synthetic metal oxides.[27] Some of these adsorbents do have drawbacks, though. For example, activated carbon is expensive despite having a large surface area.[28] There are also difficulties in its regeneration.[30] The use of agricultural materials has certain advantages such as the fact that they have highly reusable, efficient, abundant, low-cost and possess desirable functional groups for the adsorption of pollutants.[31] They have been successfully applied for the removal of heavy metals, dyes, and others. Despite these advantages, agricultural waste has clogging, separation, and decomposition issues that restrict its use on an industrial scale,[32] thus giving motivation for the search for more innovative materials that overcome these drawbacks. Among clays, bentonite is widely used in water purification because of its high surface area, high cation exchange capacity, high chemical and mechanical stabilities and efficiency for the removal of a wide range of pollutants.[33] Hence, the modification of coconut husk, an agricultural waste with bentonite was carried out. The objectives of this study were to prepare carbon materials using two inexpensive natural materials, bentonite and coconut husk, and evaluate the efficiency of the adsorbents using batch studies for the removal of three ECs under various experimental conditions. Due to their widespread usage and resistance to degradation, ciprofloxacin, tetracycline and bisphenol A have been chosen as model pollutants.

2. Materials and methods

2.1. Materials

Bisphenol A, tetracycline and ciprofloxacin were obtained from Sigma-Aldrich (St. Louis, USA). Hydrochloric acid (HCl), potassium hydroxide (KOH) and sodium hydroxide (NaOH) were obtained from Merck Chemicals (Darmstadt, Germany). All reagents were of analytical grade and were used as received.

2.2. Preparation of the bentonite–coconut husk composite (BECH)

The method of Egbedina *et al.*[21] was followed in the preparation of the adsorbents. From local markets in Ibadan, Nigeria coconut husks were purchased. Coconut husks were dried at 80 °C for 24 hours before being processed into fine powder. For the carbonization process, 1 g of coconut husk powder, 1 g of bentonite clay, 2 g of $ZnCl_2$ and 0.1 M NaOH were placed in a beaker. Before being allowed to impregnate in an oven for 24 hours at 150 °C, the mixture was stirred intermittently for 12 hours. After that, the impregnated mixture was placed in a microwave and carbonized. The resulting material was washed, dried at 60 °C for 12 hours and named BECH.

2.2.1. Chemical activation of BECH. BECH was chemically activated by soaking in 50 mL HCl and KOH separately. After 1 hour of constant agitation, the mixture was filtered. The activation products were washed with deionized water until no trace of either HCl or KOH was found. Drying was done for 24 hours at 60 °C. The activated carbons were labelled BECH-H and BECH-K for HCl and KOH activated respectively.

2.3. Characterization of BECH, BECH-H and BECH-K

The salt addition method, as reported by Adebowale *et al.*,[31] was used to establish the pH at which the adsorbents are electrically neutral (pHpzc). A scanning electron microscope (SEM) (VEGA 3 TESCAN, Brno, Czech) connected to an energy-dispersive X-ray (EDX) analyzer was used. Analysis was carried out at a voltage of 20 kV. Transmission electron microscopy (TEM) was carried out at an accelerating voltage of 200 kV. Both SEM and TEM were used to evaluate the morphological features of the adsorbents. An X-ray diffractometer (XRD) (Malvern PANalytical Ltd, The Netherlands) enabled the determination of the mineralogical composition of the adsorbents. The specific surface areas, pore volumes and pore sizes of the adsorbents were measured using nitrogen adsorption at 77 K using a Micromeritics® TriStar II Plus surface area and porosity analyzer. Fourier transform infrared (FTIR) spectroscopy was used to assess the surface chemistry of the materials using a Shimadzu FT-IR 8400S (class 1, laser product).

2.4. Batch adsorption studies

Adsorption tests were carried out by mixing 10 mL of ciprofloxacin, tetracycline and bisphenol A solutions with 50 mg of BECH, BECH-H and BECH-K in 100 mL amber glass bottles and shaking them at 150 rpm. The effects of pH, contact time and

concentration were studied and details of each study are described below. The final pollutant concentration was determined using a UV-vis spectrophotometer at wavelengths of 224.5 nm, 277.5 nm, and 365.6 nm for bisphenol A, ciprofloxacin and tetracycline respectively using a calibration curve. All of the studies were done in duplicate.

Using 40 mg L^{-1} solutions, the effect of pH on ciprofloxacin, tetracycline and bisphenol adsorption was examined. The pH was varied from 2–12 using NaOH or HCl solutions and shaken for 120 minutes at room temperature. The impact of varying contact time was examined using 40 mg L^{-1} of the pollutant at pH 7 and shaking at various intervals at room temperature. Pollutant solutions with concentrations ranging from 10 to 500 mg L^{-1} were used to study the effect of the initial concentration of pollutants.

The amounts of pollutant adsorbed (mg g^{-1}) and the adsorption efficiencies of the adsorbents were evaluated using eqn (1) and (2)

$$q_e = \frac{(C_i - C_f)V}{m} \quad (1)$$

$$\text{Adsorption efficiency} = \frac{(C_i - C_f)}{C_i} \times 100 \quad (2)$$

where C_i is the initial concentration in mg L^{-1}; C_f is the final concentration in mg L^{-1}; V is the volume of the solutions in litres; m is the dry mass of the adsorbent in grams.[8]

The adsorption kinetics were described using the kinetic equations (eqn (3) and (4)):

$$\text{Pseudo-first order: } q_t = q_e - \exp(\ln q_e - k_1 t) \quad (3)$$

$$\text{Pseudo second order: } q_t = \frac{q_e^2 k_2 t}{q_e k_2 t + 1} \quad (4)$$

where q_e and q_t stand for the amounts adsorbed at equilibrium and time, t, in mg g^{-1} respectively; k_1 is the first-order rate constant (g mg^{-1} min^{-1}), k_2 is the second-order rate constant (g mg^{-1} min^{-1}) and t is the time expressed in minutes.

Adsorption isotherms were described using adsorption models (eqn (5) and (6)).

$$\text{Freundlich: } q_e = K_F C_e^{1/n} \quad (5)$$

$$\text{Sips: } q_e = \frac{Q_s (K_s C_e)^n}{1 + (K_s C_e)^n} \quad (6)$$

C_e is the equilibrium concentration of the pollutants in solution (mg L^{-1}), K_F is an empirical constant that gives an idea of the adsorption capacity of the adsorbent, K_s is the Sips isotherm's equilibrium constant, n is the adsorption constant showing the intensity of heterogeneity of adsorption and Q_s is the Sips isotherm's adsorption capacity (mg g^{-1}).

3. Results and discussion

3.1. Characterization of BECH, BECH-H and BECH-K

The net surface charge on each adsorbent at different pH was determined through pHpzc measurement. This is important because ciprofloxacin, tetracycline and bisphenol A are known to exhibit different behaviours depending on the pH of the aqueous solution and this can result in either attraction or repulsion between the pollutants and the adsorbents.[31] The pH at the point of zero charge (pHpzc) of the adsorbents yielded values of 6.49, 2.94, and 7.13 for BECH, BECH-H and BECH-K, respectively (Fig. 1). This implies that the net surface charge on BECH, BECH-H and BECH-K will become more positive as the pH of the solution decreases below their pHpzc and become negative as the pH of the solution increases above their pHpzc. The activation of BECH with HCl resulted in a decrease in pHpzc because of the presence of H^+ from the acid used while activation with KOH resulted in an increase in the pHpzc value as a result of OH^- groups introduced to the surface of the adsorbent. This pattern is also seen when cow hoof powder was activated with an acid and alkali.[34] Acid activation also resulted in a decrease of pHpzc (*i.e.* from 5.22 to 4.6) and alkali treatment resulted in an increase (5.22 to 7).

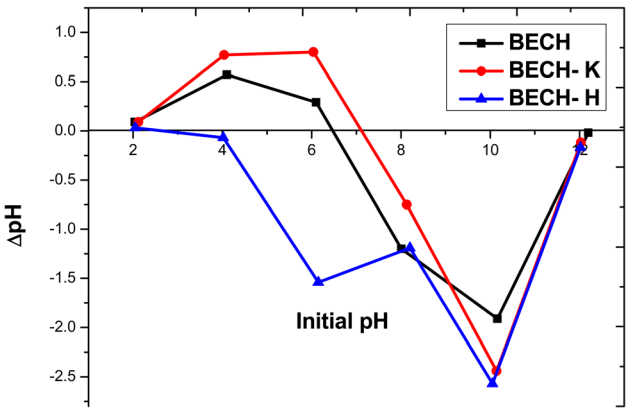

Fig. 1 pHpzc plots of BECH, BECH-H and BECH-K.

Fig. 2 displays the FTIR spectra of BECH, BECH-H, and BECH-K. The spectra of the adsorbents displayed similar bands to bentonite though marked shifts in the absorption bands were

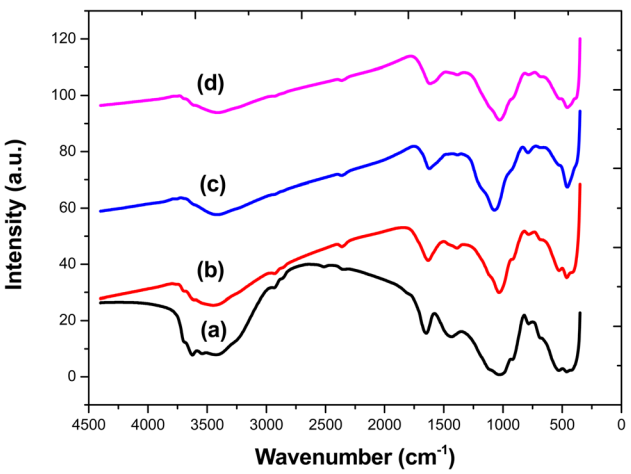

Fig. 2 FTIR spectra of (a) bentonite, (b) BECH, (c) BECH-H and (d) BECH-K.

observed. The peak at 1042 cm^{-1}, corresponding to the stretching vibration of Si–O in bentonite was found at 1034 cm^{-1}, 1067 cm^{-1} and 1026 cm^{-1} for BECH, BECH-H and BECH-K, respectively. While the peaks detected at 526 cm^{-1} and 444 cm^{-1} for bentonite are attributed to the asymmetric stretching vibrations of Si–O–Al and Si–O–Si, respectively, the peak at 3435 cm^{-1} for bentonite is attributed to the absorbance of the O–H functional groups of Al–OH on SMC.[33] These latter bands were not seen in the modified adsorbents, possibly masked by the interaction with the biomass thus indicative of interactions between the bentonite and the coconut husk. The reduced intensity of the external O–H stretching band at 3632 cm^{-1} found in bentonite and absent in the composites is attributed to heat treatment during the preparation of SMC. The band at 460 cm^{-1} for BECH, BECH-H and BECH-K confirms the presence of ZnO[21] resulting from the interaction between $ZnCl_2$ and NaOH during their preparation.

Fig. 3 depicts the SEM images of BECH, BECH-H and BECH-K at a magnification of 50 μm. The surfaces have irregular, heterogeneous pores with uneven diameters, as shown in the SEM micrographs. BECH's image revealed fewer pores than BECH-H and BECH-K. The particles are also distributed heterogeneously, differing in size and form. On activation, more

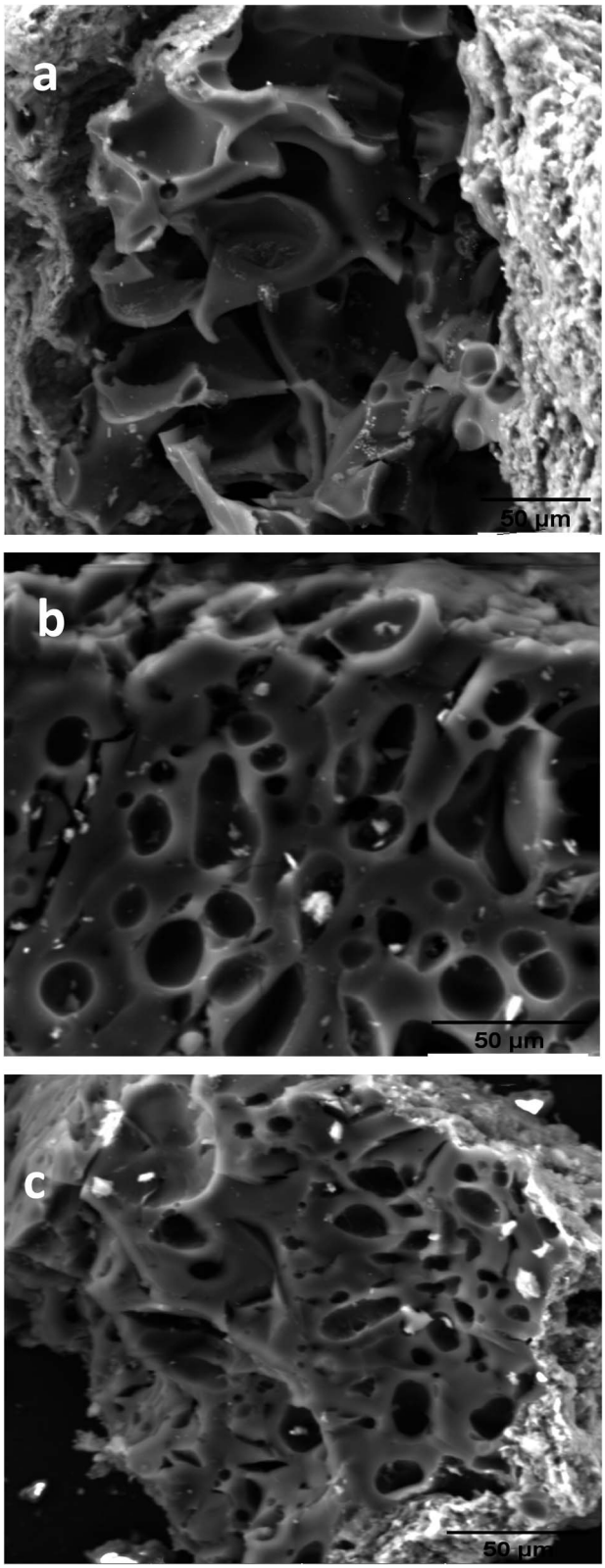

Fig. 3 SEM images of (a) BECH, (b) BECH-H and (c) BECH-K.

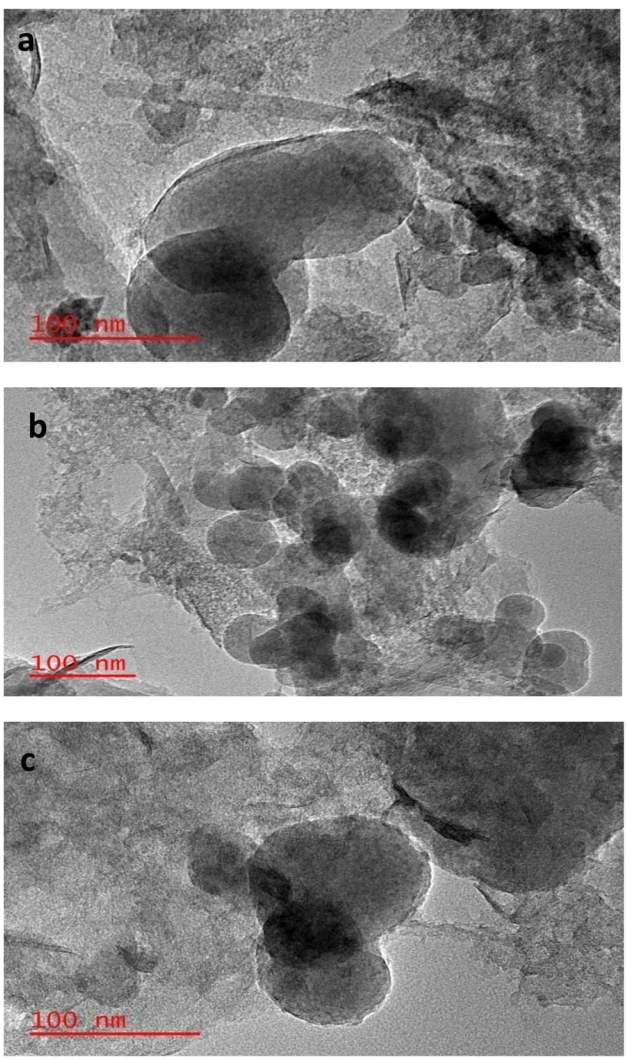

Fig. 4 HR-TEM micrographs of (a) BECH, (b) BECH-H and (c) BECH-K.

pores appear to be more visible. Activation frequently results in enhanced porosity because the amorphous material that normally clogs the pore network in adsorbents is easily removed, making the already-existing pores accessible.[34]

HR-TEM was used to further characterize the adsorbents (Fig. 4), which confirmed the formation and aggregation of ZnO on the surface of the adsorbents. This is indicated by the darker layer on the TEM images.

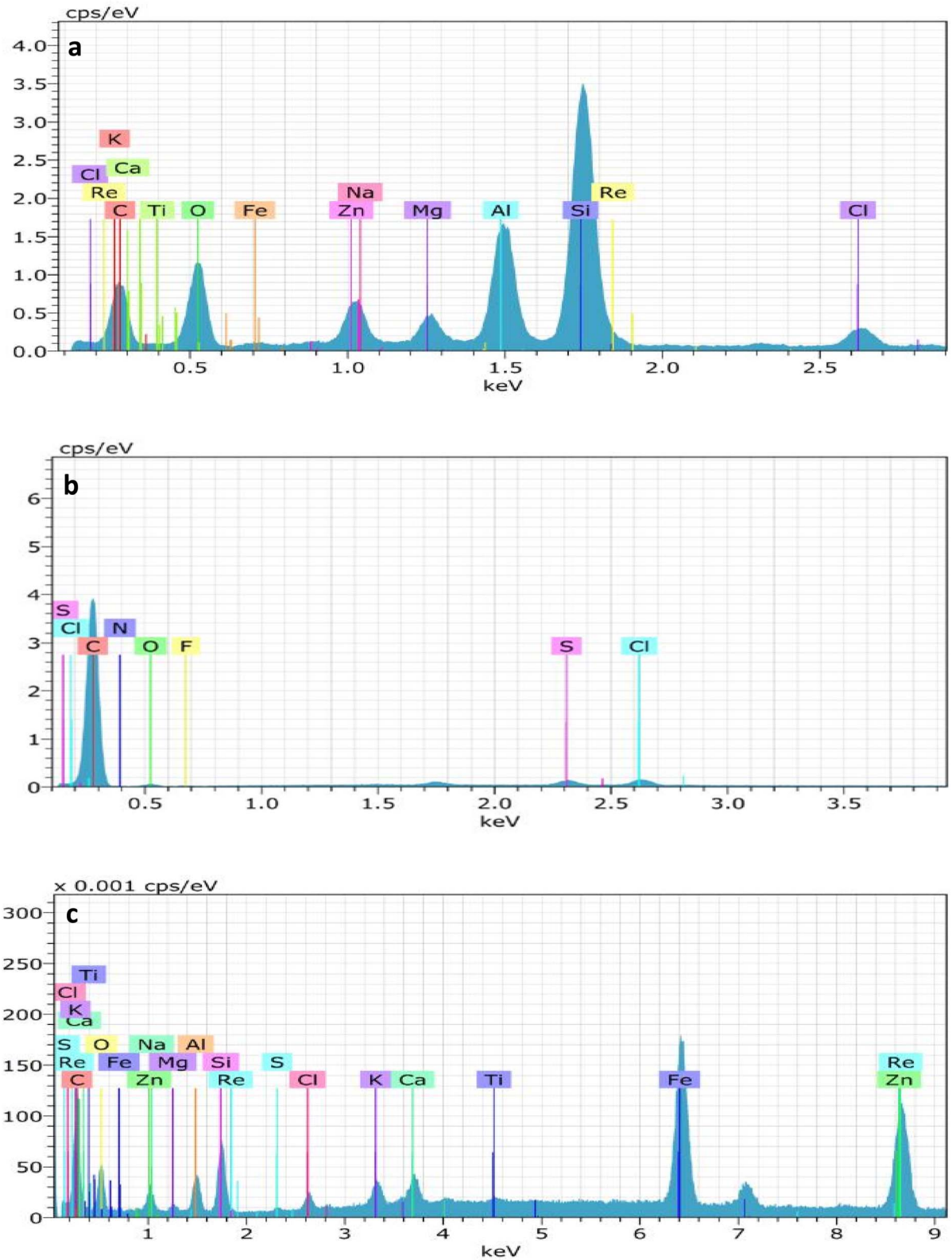

Fig. 5 EDX spectra of (a) BECH, (b) BECH-H and (c) BECH-K.

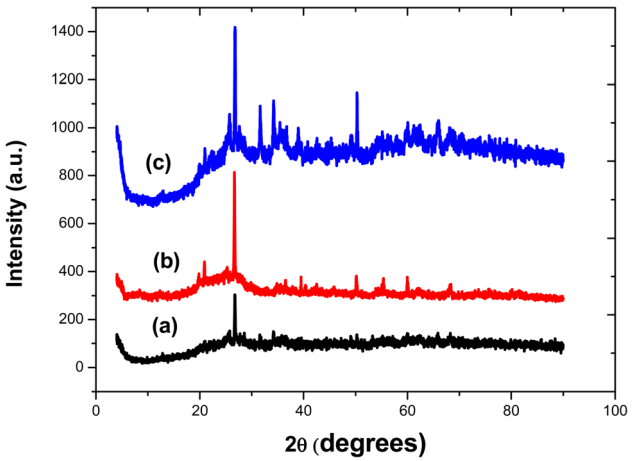

Fig. 6 XRD spectra of (a) BECH, (b) BECH-H and (c) BECH-K.

EDX analysis (Fig. 5) shows that BECH (47%), BECH-H (91%) and BECH-K (56%) contain carbon as opposed to bentonite clay. This demonstrates the successful carbonization of bentonite and coconut husk. Furthermore, the activation of BECH resulted in a higher amount of carbon in BECH-H and BECH-K, showing that activation improved the surface properties of BECH. The spectra also show the presence of Zn in the samples showing that Zn was not washed away during the preparation of the adsorbents. Silicon (Si), iron (Fe), oxygen (O), calcium (Ca), and magnesium (Mg) are among the other elements attributed to contributions from biomass and clay.

The XRD spectra of the adsorbents are shown in Fig. 6. The amorphous character of the adsorbents, which is typical of carbon, is shown by the nature of the diffractogram. The diffraction pattern of BECH shows peaks at 2θ of 4.01°, 26.97°, 42.26°, 50.23°, 59.98° and 68.22°. These peaks are found in BECH-H at 2θ of 4.42°, 26.70°, 42.60°, 50.25°, 59.98°, and 68.39° and in BECH-K at 2θ of 4.13°, 26.81°, 42.59°, 50.29° and 68.77°. These peaks correspond to the presence of quartz, montmorillonite and calcite and are typical of bentonite.[35,36] This demonstrates that though biomass and bentonite had interacted, this interaction did not affect the mineralogical structure of the parent clay material. The Debye–Scherrer equation (eqn (7)) was used to calculate the crystallite size and the L_c of the adsorbents using the full width at maximum height (FWMH).

$$L_c = \frac{k\lambda}{\beta_{002}\cos\theta_{002}} \quad (7)$$

where L_c is the estimated crystallite size; k is the Scherrer constant which is 0.9; λ is the X-ray wavelength of radiation for Cu-Kα (0.154 nm); β is the full-width at half maximum in radians (obtained by comparing relative area ratios after fitting Gaussian peaks); θ is the diffraction angle.[21] The crystallite sizes for BECH, BECH-H, and BECH-K were found to be 8.1, 8.1, and 6.9 nm, respectively.

The nitrogen adsorption–desorption isotherms of BECH, BECH-H and BECH-K are shown in Fig. 7. The BET surface area of BECH, BECH-H and BECH-K is 284, 456 and 312 $m^2\ g^{-1}$ respectively. These values are higher than that obtained for pristine bentonite (74 $m^2\ g^{-1}$). The surface areas of the activated adsorbents, BECH-H and BECH-K, are higher than that of BECH showing that activation improved the surface properties of BECH. The surface areas of the three adsorbents are also higher when compared to those of other bentonite-based adsorbents.[33,37] The large specific surface areas obtained for the three

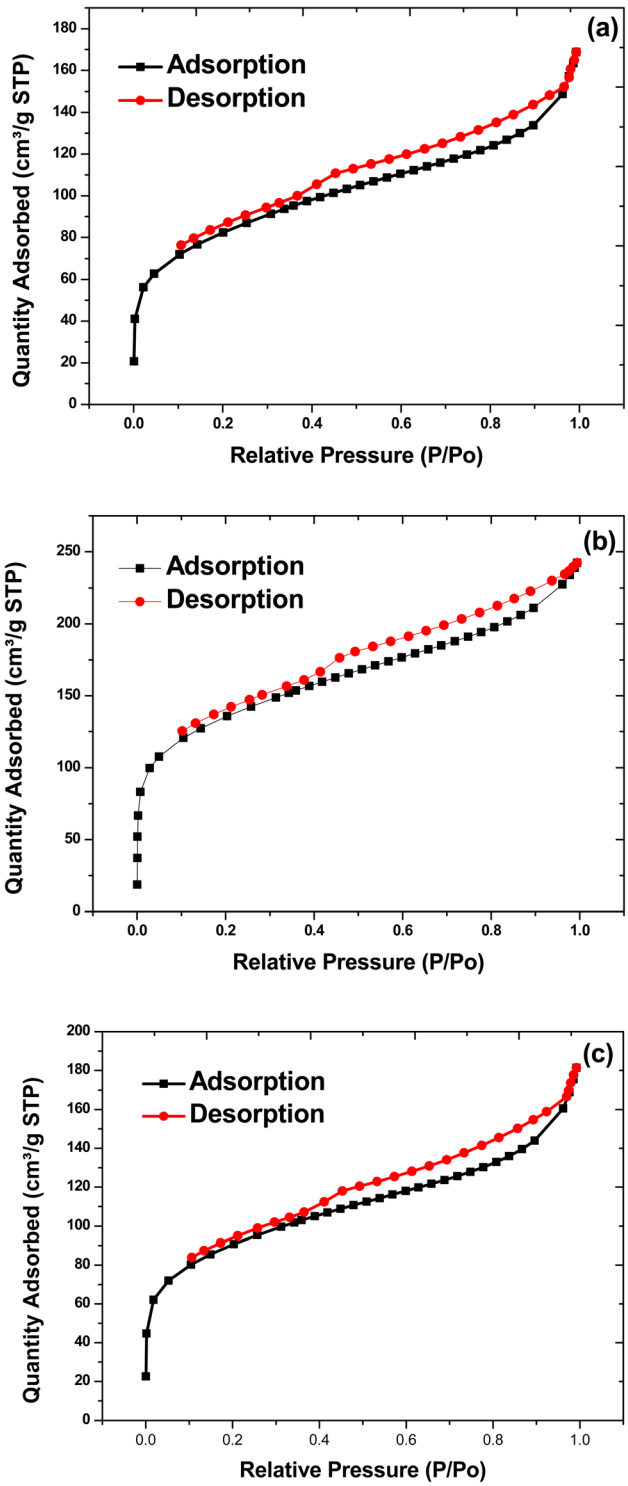

Fig. 7 Nitrogen adsorption–desorption isotherm of (a) BECH, (b) BECH-H and (c) BECH-K.

Table 1 Surface properties of bentonite, BECH, BECH-H and BECH-K

	Surface area (m^2 g^{-1})	Pore size (nm)	Pore volume (cm^3 g^{-1})
Bentonite	73.87	9.76	0.18
BECH	284.14	3.68	0.26
BECH-H	456.17	3.29	0.38
BECH-K	311.97	3.59	0.28

adsorbents make them potentially good adsorbents for the removal of the target pollutants. Additional surface characteristics of the adsorbents derived from BET analysis are displayed in Table 1. The pore sizes of the adsorbents prepared were seen to be smaller than that of the pristine parent clay. This size reduction could be attributed to the coconut husk incorporated into it, which resulted in a reduction in pore size.

3.2. Batch adsorption

3.2.1. pH effect. The properties of both the adsorbents and the adsorbate are affected by pH, making it a crucial parameter to be studied. The effect of pH on ciprofloxacin, tetracycline, and bisphenol A adsorption is shown in Fig. 8. Ciprofloxacin adsorption on BECH (Fig. 8a) increased up to pH 10. As the pH increased, the adsorption capacity began to fall sharply. BECH has a pHpzc of 6.49 (Fig. 1). Below this pH, the surface of this adsorbent is positively charged. In contrast, ciprofloxacin exists as a neutral molecule between pH 6.1 and 8.9. Below 6.1, it exists as a cation and an anion above pH 9.[8] Based on this knowledge, it is expected that adsorption will be low at pH below 6 due to electrostatic interactions, as both the adsorbent and the adsorbate are positively charged. This was not the case as adsorption increased steadily at a pH lower than 6. This increase in adsorption could be attributed to the hydrophobicity of ciprofloxacin which suppressed electrostatic interactions.[38] Furthermore, ciprofloxacin is anionic at a pH higher than 9, whereas the adsorbent is negatively charged. Hydrophobic character is lowered with the formation of anions, and adsorption will be reduced at alkaline pH.[39] This is responsible for the decrease in ciprofloxacin adsorption from pH 10. This shows that the primary mechanism of interaction between ciprofloxacin and BECH is hydrophobic interaction. Similar patterns were seen with ciprofloxacin adsorption on BECH-H, which showed a decrease in adsorption from pH 2 to 4, and then an increase in adsorption with a peak at pH 8. BECH-K on ciprofloxacin showed increased adsorption up to pH 4. BECH-H with a pHpzc of 2.94 demonstrated an increase in adsorption when pH went from acidic to alkaline conditions for tetracycline adsorption (Fig. 8b). On the other hand, BECH-K demonstrated a reduction in adsorption as pH increased. The behaviours of both adsorbents suggest that hydrophobic interactions were the main driving force in the adsorption and rule out electrostatic interactions as the major mechanism of adsorption. These results corroborate studies that describe hydrophobic interactions as the main driving force between aromatic organics and carbon-based adsorbents.[40]

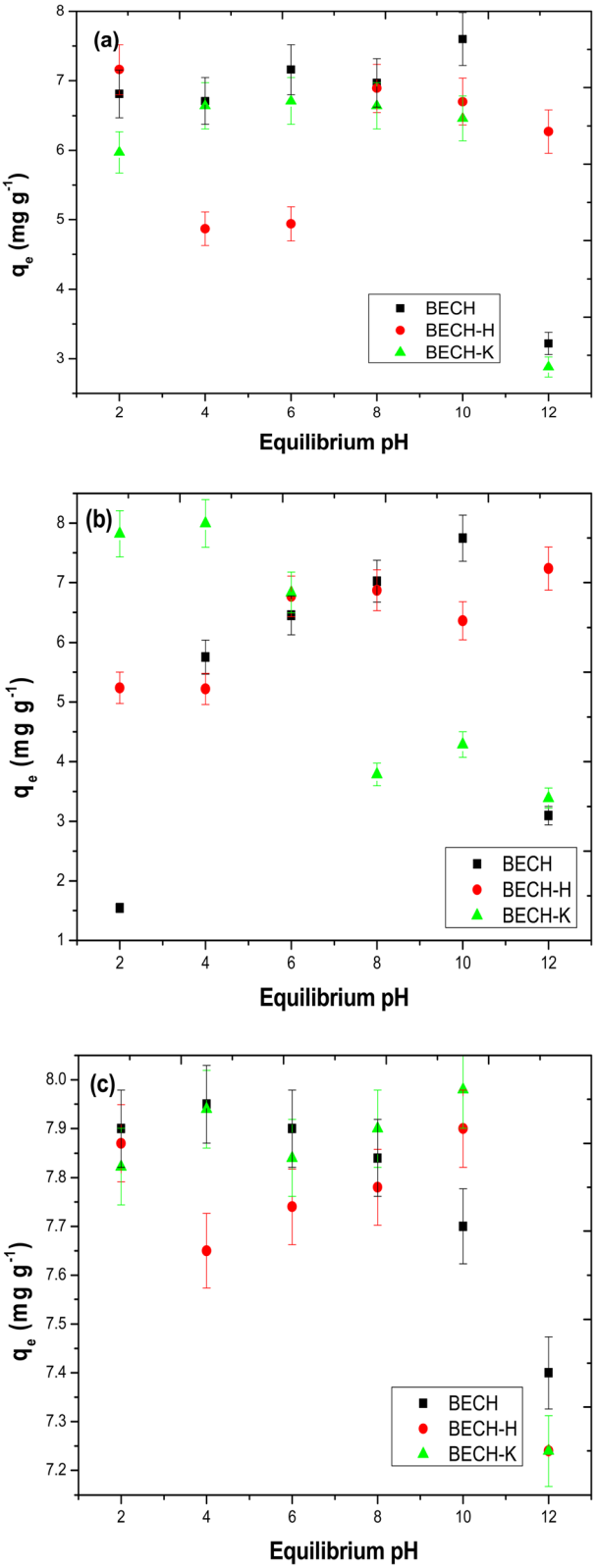

Fig. 8 Effect of pH on the adsorption of (a) ciprofloxacin, (b) tetracycline and (c) bisphenol A (adsorbent mass – 50 mg; pollutant concentration – 40 mg L^{-1}; contact time – 120 min).

Table 2 Kinetic model parameters for the adsorption of ciprofloxacin, tetracycline and bisphenol A onto BECH, BECH-H and BECH-K

Kinetic model	Parameters	BECH			BECH-H			BECH-K		
		Ciprofloxacin	Tetracycline	Bisphenol A	Ciprofloxacin	Tetracycline	Bisphenol A	Ciprofloxacin	Tetracycline	Bisphenol A
Pseudo-first order	q_e (mg g^{-1})	7.154	5.777	7.490	7.073	5.931	7.408	7.083	6.706	7.283
	k_1 (min^{-1})	1.132	1.336	0.874	1.178	0.892	1.259	1.078	0.441	1.166
	Error	0.617	0.152	0.353	0.400	0.463	0.295	0.577	0.762	0.409
Pseudo-second order	q_e (mg g^{-1})	7.374	5.871	7.781	7.247	6.198	7.576	7.244	7.124	7.488
	k_2 (g mg^{-1} min^{-1})	0.378	0.854	0.243	0.461	0.28	0.501	0.445	0.112	0.794
	Error	0.550	0.103	0.175	0.258	0.342	0.202	0.230	0.663	0.139

Table 3 Adsorption isotherm model parameters for the adsorption of ciprofloxacin, tetracycline and bisphenol A onto BECH, BECH-H and BECH-K

Kinetic model	Parameters	BECH			BECH-H			BECH-K		
		Ciprofloxacin	Tetracycline	Bisphenol A	Ciprofloxacin	Tetracycline	Bisphenol A	Ciprofloxacin	Tetracycline	Bisphenol A
Freundlich	K_F	4.946	16.155	9.35×10^{-4}	2.068	1.496	0.835	1.805	0.059	2.665
	n	1.504	0.999	0.248	1.089	0.634	0.593	0.979	0.428	0.815
	R^2	0.894	0.999	0.987	0.919	0.920	0.953	0.807	0.871	0.994
	Error	11.326	2.86×10^{-8}	4.446	11.148	10.223	8.522	16.463	13.974	2.904
Sips	Q_s	199.669	281.673	183.565	90.782	79.544	304.588	118.997	95.330	472.999
	K_s	1.4×10^{-4}	6.89×10^{-3}	5.8×10^{-2}	1.2×10^{-3}	6.204	4.28×10^{-3}	6.7×10^{-2}	5.4×10^{-3}	3.15×10^{-2}
	n_s	0.678	1.045	6.01	0.945	9.076	1.69	4.499	2.348	1.418
	R^2	0.893	0.999	0.991	0.945	0.906	0.952	0.953	0.871	0.996
	Error	12.689	0.0662	4.259	11.445	13.516	9.554	9.055	15.637	2.775

The adsorption of tetracycline on BECH rose gradually up to pH 10; at this pH, tetracycline and BECH are both negatively charged, resulting in a decrease attributed to electrostatic repulsion. Due to electrostatic repulsion brought about by the positive charges of the adsorbent and adsorbate, reduced adsorption was also seen at lower pH. Adsorption capacity rose even more as tetracycline became less positive, moving towards neutrality. This suggests that electrostatic interaction may be the dominant mode of interaction. The result obtained for tetracycline on BECH was similar to what Li *et al.*[41] reported. The adsorption of tetracycline on BECH-H was found to increase while that on BECH-K decreases over the range of pH studied.

When the pH is less than 8, bisphenol A is found in its molecular form. The initial deprotonation of BPA occurs at pH 8, whereas the second occurs around pH 9.[42] Adsorption peaked at pH 10 for BECH-K (Fig. 8c), while that of BECH was at pH 4 after which a gradual drop in adsorption occurred. BECH is positively charged at this pH of 4, whereas bisphenol A is neutral. Though less energetic, neutral bisphenol A can interact with adsorbents in this state (positively charged) *via* oxygen atoms that can give electrons.[39] On the other hand, BECH-H exhibited an adsorption pattern that was identical to that of ciprofloxacin removal on BECH. This behaviour is similar to those reported in the literature for the adsorption of BPA on other adsorbent materials.[43]

3.2.2. Adsorption kinetics. Adsorption kinetics were examined to predict the rate and mechanism of adsorption. The kinetic parameters for the adsorption models used to study the experimental data of the adsorption of the pollutants onto the three adsorbents are shown in Table 2. The findings show that pollutant adsorption occurred rapidly on all the adsorbents. Fast adsorption is usually associated with a high affinity between pollutants and adsorbents. The model that most accurately describes the experimental data was determined using the relative standard error. The lower the value of error, the greater the fitting of the adsorption data to the model. From Table 2, the pseudo-second-order model had the lowest error value for the adsorption of ciprofloxacin, tetracycline and bisphenol A on the three adsorbents. The pseudo-second-order kinetic model proposes chemisorption (*i.e.*, interactions in which electrons are either shared or transferred between the pollutants and the adsorbents govern adsorption) as the rate-determining step.[44] If k_1 is higher than k_2, this may indicate simultaneous internal diffusion and surface adsorption of adsorbates.[45] In this study, the k_1 values for all the adsorption were found to be greater than the k_2 values showing that more than one mechanism was involved in the adsorption.

3.2.3. Adsorption isotherms. The experimental data obtained for this study were analyzed using the non-linear equations of the Freundlich and Sips isotherm models. Table 3 summarizes the values of the model parameters, as well as the coefficient of determination (R^2) and relative standard error. The Sips model best described the adsorption equilibrium of data based on the R^2 and RSE values shown in this table. This model predicts that the active sites of the adsorbents do not possess the same energy.[46] These findings revealed that the adsorption obeyed the predictions of the Freundlich isotherm at lower concentrations and those of the Langmuir isotherm at higher concentrations illustrating that both physical and chemical interactions were involved in the process (Fig. 9). It also confirms the result obtained from the kinetic data modelling, which suggested that more than one mechanism of interaction was involved.

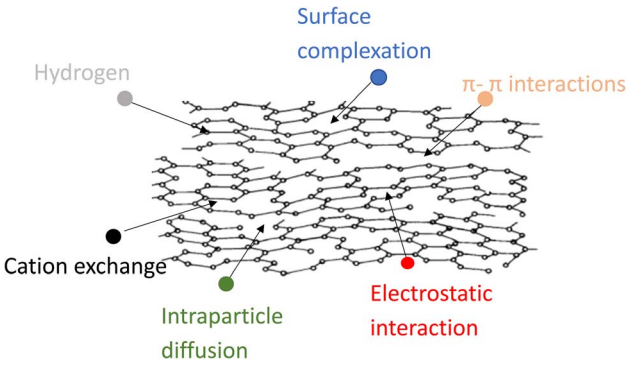

Fig. 9 Schematic diagram illustrating the plausible adsorption mechanisms.

The maximum adsorption capacity (q_{max}) computed for ciprofloxacin using the Sips model is 199.67 mg g^{-1}, 118.99 mg g^{-1} and 90.79 mg g^{-1} for BECH, BECH-H, and BECH-K, respectively. Tetracycline adsorption yielded q_{max} values of 281.67, 79.54 and 95.33 mg g^{-1} for BECH, BECH-H and BECH-K, respectively, while bisphenol A adsorption yielded 183.57, 472.9 and 304.58 mg g^{-1} for BECH, BECH-H, and BECH-K, respectively. For bisphenol A, BECH-H and BECH-K showed the greatest affinity for bisphenol A with BECH-H having the highest adsorption capacity (472.9 mg g^{-1}). Conversely, BECH had the greatest preference for ciprofloxacin (199.7 mg g^{-1}) and tetracycline (281.7 mg g^{-1}). These differences in adsorption capacity can be attributed to the nature of the adsorbent *i.e.*, the number of adsorption sites (surface area), the porosity and the size of the pores. The affinity of different adsorbents and the size of the pores concerning the molecular size of adsorbates could lead to differences in adsorption capacities obtained for different contaminants on the same adsorbent.

4. Conclusion

Bentonite clay–coconut husk composites (BECH) were prepared and further activated with KOH and HCl to give BECH-K and BECH-H. The functional groups, elemental compositions, and morphology of the three adsorbents were determined through characterization. The results obtained showed that BECH-H has the highest specific surface area of the three adsorbents. According to adsorption studies, electrostatic and hydrophobic interactions may have been crucial in the adsorption of these emerging pollutants. The adsorption kinetics and isotherms were best explained by the Sips model and the pseudo-second-order model, respectively, thus implying that the adsorptions took place on heterogeneous active sites with different mechanisms occurring at the different sites. The maximum

adsorption capacities ranged from 80 to 473 mg g^{-1}. BECH, BECH-K and BECH-H had high removal capabilities for ciprofloxacin, bisphenol A and tetracycline indicating that they all have the potential for removing these pollutants from industrial wastewater.

Author contributions

Abisola Egbedina: investigation, methodology, and writing – original draft. Simisola Odejobi: investigation. Babatunde Akinbile: investigation. Abayneh Ambushe: resources and investigation. Bamidele I. Olu-Owolabi: conceptualization, investigation, validation, and writing – review & editing. Kayode Adebowale: conceptualization, methodology, writing – review & editing, and project administration.

Conflicts of interest

The authors declare that they have no known competing interests.

References

1 A. O. Egbedina, B. I. Olu-Owolabi and K. O. Adebowale, Batch and continuous fixed-bed adsorption of antibiotics from aqueous solution using stearic acid-activated carbon composite, *Energy Ecol. Environ.*, 2023, **8**, 129–140, DOI: 10.1007/s40974-023-00268-7.

2 U. Wazir and K. Mokbel, Bisphenol A: a concise review of the literature and a discussion of health and regulatory implications, *In Vivo*, 2019, **33**(5), 1421–1423, DOI: 10.21873/invivo.11619.

3 É. Ujaczki, V. Stark-Rogel, M. Olbrich, M. Fuetsch and J. Backmann, Experiences and consequences of phasing out substances of concern in a multinational healthcare company, *Environ. Sci. Eur.*, 2022, **34**(1), 101, DOI: 10.1186/s12302-022-00678-0.

4 A. Gałązka and U. Jankiewicz, Endocrine Disrupting Compounds (Nonylphenol and Bisphenol A)-Sources, Harmfulness and Laccase-Assisted Degradation in the Aquatic Environment, *Microorganisms*, 2022, **10**(11), 2236, DOI: 10.3390/microorganisms10112236.

5 C. M. Sijaona, P. M. Faith, S. Bjarne and H. M. Robinson, Pollution by endocrine disrupting estrogens in aquatic ecosystems in Morogoro urban and peri-urban areas in Tanzania, *Afr. J. Environ. Sci. Technol.*, 2017, **11**(2), 122–131, DOI: 10.5897/ajest2016.2234.

6 A. A. Borghi and M. S. A. Palma, Tetracycline: production, waste treatment and environmental impact assessment, *Braz. J. Pharm. Sci.*, 2014, **50**(1), 25–40, DOI: 10.1590/S1984-82502011000100003.

7 F. Ahmad, D. Zhu and J. Sun, Environmental fate of tetracycline antibiotics: degradation pathway mechanisms, challenges, and perspectives, *Environ. Sci. Eur.*, 2021, **33**(1), 64, DOI: 10.1186/s12302-021-00505-y.

8 A. O. Egbedina, S. Ibhafidon, B. J. Akinbile, A. A. Ambushe, B. I. Olu-Owolabi and K. O. Adebowale, Catalytic transformation of coconut husk into single-crystal graphite and its application for the removal of antibiotics from wastewater, *Chem. Eng. Res. Des.*, 2022, **188**, 96–104, DOI: 10.1016/j.cherd.2022.09.042.

9 M. P. C. Mora-Gamboa, S. M. Rincón-Gamboa, L. D. Ardila-Leal, R. A. Poutou-Piñales, A. M. Pedroza-Rodríguez and B. E. Quevedo-Hidalgo, Impact of Antibiotics as Waste, Physical, Chemical, and Enzymatical Degradation: Use of Laccases, *Molecules*, 2022, **27**(14), 4436, DOI: 10.3390/molecules27144436.

10 N. Hanna, A. J. Tamhankar and C. Stålsby Lundborg, Antibiotic concentrations and antibiotic resistance in aquatic environments of the WHO Western Pacific and South-East Asia regions: a systematic review and probabilistic environmental hazard assessment, *Lancet Planet. Health*, 2023, **7**(1), e45–e54, DOI: 10.1016/S2542-5196(22)00254-6.

11 M. J. Ahmed and B. H. Hameed, Removal of emerging pharmaceutical contaminants by adsorption in a fixed-bed column: a review, *Ecotoxicol. Environ. Saf.*, 2018, **149**, 257–266, DOI: 10.1016/j.ecoenv.2017.12.012.

12 A. Inyinbor, B. Adebesin, A. Oluyori, T. Adelani-Akande, A. Dada and T. Oreofe, Impact Water Pollution: Effects, Prevention, and Climatic Impact, in *Water Challenges of an Urbanizing World*, ed. M. Glavan, IntechOpen, United Kingdom, 2018, pp. 3–53, DOI: 10.5772/intechopen.7201837.

13 R. Kumar, M. Qureshi, D. K. Vishwakarma, *et al.*, A review on emerging water contaminants and the application of sustainable removal technologies, *Case Stud. Chem. Environ. Eng.*, 2022, **6**, 100219, DOI: 10.1016/j.cscee.2022.100219.

14 P. Krasucka, B. Pan, Y. Sik Ok, D. Mohan, B. Sarkar and P. Oleszczuk, Engineered biochar – a sustainable solution for the removal of antibiotics from water, *Chem. Eng. J.*, 2021, **405**(August 2020), 126926, DOI: 10.1016/j.cej.2020.126926.

15 H. Zhan, Y. Wang, X. Mi, Z. Zhou, P. Wang and Q. Zhou, Effect of graphitic carbon nitride powders on adsorption removal of antibiotic resistance genes from water, *Chin. Chem. Lett.*, 2020, **31**(10), 2843–2848, DOI: 10.1016/j.cclet.2020.08.015.

16 M.-F. N. Secondes, V. Naddeo, V. Belgiorno and F. Ballesteros, Removal of emerging contaminants by simultaneous application of membrane ultrafiltration, activated carbon and ultrasonic irradiation, *J. Hazard. Mater.*, 2014, **264**, 342–349.

17 J. Wang and M. Zhang, Adsorption Characteristics and Mechanism of Bisphenol A by Magnetic Biochar, *Int. J. Environ. Res. Public Health*, 2020, **17**, 1075, DOI: 10.3390/ijerph17031075.

18 S. Ghosh, A. Othmani, A. Malloum, *et al.*, Removal of mercury from industrial effluents by adsorption and advanced oxidation processes: a comprehensive review, *J. Mol. Liq.*, 2022, **367**, 120491, DOI: 10.1016/j.molliq.2022.120491.

19 D. A. Gkika, A. C. Mitropoulos and G. Z. Kyzas, Why reuse spent adsorbents? The latest challenges and limitations,

Sci. Total Environ., 2022, **822**, 153612, DOI: 10.1016/j.scitotenv.2022.153612.

20 V. Rakic, V. Rac, M. Krmar, O. Otman and A. Auroux, The adsorption of pharmaceutically active compounds from aqueous solutions onto activated carbon, *J. Hazard. Mater.*, 2015, **282**, 141–149.

21 A. O. Egbedina, K. O. Adebowale, B. I. Olu-Owolabi, E. I. Unuabonah and M. O. Adesina, Green synthesis of ZnO coated hybrid biochar for the synchronous removal of ciprofloxacin and tetracycline in wastewater, *RSC Adv.*, 2021, **11**(30), 18483–18492, DOI: 10.1039/d1ra01130h.

22 A. Gil, N. Taoufik, A. M. García and S. A. Korili, Comparative removal of emerging contaminants from aqueous solution by adsorption on activated carbon, *Environ. Technol.*, 2018, **40**(23), 3017–3030, DOI: 10.1080/09593330.2018.1464066.

23 G. Gopal, C. Natarajan and A. Mukherjee, Adsorptive removal of fluoroquinolone antibiotics using green synthesized and highly efficient Fe clay cellulose-acrylamide beads, *Environ. Technol. Innovation*, 2022, **28**, 102783, DOI: 10.1016/j.eti.2022.102783.

24 C. Levard, K. Hamdi-Alaoui, I. Baudin, *et al.*, Silica-clay nanocomposites for the removal of antibiotics in the water usage cycle, *Environ. Sci. Pollut. Res.*, 2021, **28**(6), 7564–7573, DOI: 10.1007/s11356-020-11076-5.

25 D. Nayyar, M. A. Shailkh and T. Nawaz, Remediation of Emerging Contaminants by Naturally Derived Adsorbents, in *New Trends in Emerging Environmental Contaminants*, ed. S. Singh, A. K. Agarwal, T. Gupta and S. M. Maliyekkal, Springer, 2022, pp. 225–260, DOI: 10.1007/978-981-16-8367-1_11.

26 S. Tai, Y. Li, L. Yang, *et al.*, Magnetic-Transition-Metal Oxides Modified Pollen-Derived Porous Carbon for Enhanced Absorption Performance, *Int. J. Environ. Res. Public Health*, 2022, **19**(24), 16740, DOI: 10.3390/ijerph192416740.

27 M. M. Bade, A. A. Dubale, D. F. Bebizuh and M. Atlabachew, Highly Efficient Multisubstrate Agricultural Waste-Derived Activated Carbon for Enhanced CO_2 Capture, *ACS Omega*, 2022, **7**(22), 18770–18779, DOI: 10.1021/acsomega.2c01528.

28 M. Grassi, G. Kaykioglu and V. Belgiorno, Removal of Emerging Contaminants from Water and Wastewater by Adsorption Process, in *Emerging Compounds Removal from Wastewater, Natural and Solar Based Treatments*, ed. G. Lofrano, SpringerBriefs, 2012, pp. 15–38, DOI: 10.1007/978-94-007-3916-1.

29 K. Ortíz-martínez, D. V. Valentin and A. J. Hernandez-Maldonado, Adsorption of Contaminants of Emerging Concern from Aqueous Solutions using Cu^{2+} Amino Grafted SBA-15 Mesoporous Silica: Multi-Component and Metabolites Adsorption, *Ind. Eng. Chem. Res.*, 2018, **57**(18), 6426–6439, DOI: 10.1021/acs.iecr.7b05168.

30 E. Abu-Danso, A. Bagheri and A. Bhatnagar, Facile functionalization of cellulose from discarded cigarette butts for the removal of diclofenac from water, *Carbohydr. Polym.*, 2019, **219**, 46–55, DOI: 10.1016/j.carbpol.2019.04.090.

31 K. Adebowale, A. Egbedina and B. Shonde, Adsorption of lead ions on magnetically separable - Fe_3O_4 watermelon composite, *Appl. Water Sci.*, 2020, **10**, 225, DOI: 10.1007/s13201-020-01307-y.

32 A. Ahmadi, R. Foroutan and H. Esmaeili, The role of bentonite clay and bentonite clay @ $MnFe_2O_4$ composite and their physico-chemical properties on the removal of Cr(III) and Cr(VI) from aqueous media, *Environ. Sci. Pollut. Res.*, 2020, **27**, 14044–14057.

33 F. K. Katsaros, T. A. Steriotis, A. K. Stubos, N. K. Kanellopoulos and S. R. Tennison, Effect of activation process on resin-based activated carbons, in *Studies in Surface Science and Catalysis*, ed. P. L. Llewellyn, F. Rodriquez-Reinoso, J. Rouqerol and N. Seaton, Elsevier B.V., 2007, vol. 160, pp. 599–606.

34 S. L. Abdullahi and A. A. Audu, Comparative Analysis on Chemical Composition of Bentonite Clays Obtained from Ashaka and Tango Deposits in Gombe State, Nigeria, *ChemSearch J.*, 2017, **8**(2), 35–40.

35 C. De Oliviera, M. Rocha, A. Da Silva and L. Bertolino, Characterization of bentonite clays from Cubati, Paraiba (Northeast of Brazil), *Ceramica*, 2016, **62**, 272–277.

36 S. Qiao, Q. Hu, F. Haghseresht, X. Hu, G. Qing and M. Lu, An investigation on the adsorption of acid dyes on the bentonite-based composite adsorbent, *Sep. Purif. Technol.*, 2009, **67**, 218–225, DOI: 10.1016/j.seppur.2009.03.012.

37 J. Wang, B. Chen and B. Xing, Wrinkles and Folds of Activated Graphene Nanosheets as Fast and Efficient Adsorptive Sites for Hydrophobic Organic Contaminants, *Environ. Sci. Technol.*, 2016, **50**(7), 3798–3808, DOI: 10.1021/acs.est.5b04865.

38 K. K. Katibi, K. F. Yunos, H. C. Man, A. Z. Aris, M. Z. Mohd Nor and R. S. Aziz, An Insight into a Sustainable Removal of Bisphenol A from Aqueous Solution by Novel Palm Kernel Shell Magnetically Induced Biochar: Synthesis, Characterization, Kinetic, and Thermodynamic Studies, *Polymers*, 2021, **13**(21), 3781.

39 K. Ouyang, C. Zhu, Y. Zhao, L. Wang, S. Xie and Q. Wang, Adsorption Mechanism of Magnetically Separable Fe_3O_4/Graphene Oxide Hybrids, *Appl. Surf. Sci.*, 2015, **355**, 562–569, DOI: 10.1016/j.apsusc.2015.07.109.

40 A. N. Li, L. Zhou, X. Jin, G. Owens and Z. Chen, Simultaneous removal of tetracycline and oxytetracycline antibiotics from wastewater using a ZIF-8 metal organic-framework, *J. Hazard. Mater.*, 2019, **366**, 563–572, DOI: 10.1016/j.jhazmat.2018.12.047.

41 M. Li, Y. Liu, S. Liu, *et al.*, Performance of magnetic graphene oxide/diethylenetriaminepentaacetic acid nanocomposite for the tetracycline and ciprofloxacin adsorption in single and binary systems, *J. Colloid Interface Sci.*, 2018, **521**, 150–159, DOI: 10.1016/j.jcis.2018.03.003.

42 K. O. Adebowale and A. O. Egbedina, Facile green synthesis of bio-carbon material from eggshells and its application for the removal of bisphenol A and 2,4,6-trichlorophenol from water, *Environ. Nanotechnol., Monit. Manage.*, 2022, **17**, 100622, DOI: 10.1016/j.enmm.2021.100622.

43 J. Heo, Y. Yoon, G. Lee, Y. Kim, J. Han and C. Min, Enhanced adsorption of bisphenol A and sulfamethoxazole by a novel magnetic $CuZnFe_2O_4$ – biochar composite, *Bioresour.*

Technol., 2019, **281**, 179–187, DOI: 10.1016/j.biortech.2019.02.091.

44 I. Nica, C. Zaharia and D. Suteu, Hydrogel Based on Tricarboxi-Cellulose and Poly(Vinyl Alcohol) Used as Biosorbent for Cobalt Ions Retention, *Polymers*, 2021, **19**(9), 1444.

45 M. F. Mubarak, A. M. G. Mohamed, M. Keshawy, T. A. elMoghny and N. Shehata, Adsorption of heavy metals and hardness ions from groundwater onto modified zeolite: batch and column studies, *Alexandria Eng. J.*, 2022, **61**(6), 4189–4207, DOI: 10.1016/j.aej.2021.09.041.

46 G. Varank, A. Demir, K. Yetilmezsoy, S. Top, E. Sekman and M. S. Bilgili, Removal of 4-nitrophenol from aqueous solution by natural low-cost adsorbents, *Indian J. Chem. Technol.*, 2012, **19**, 7–25.